Fish and Shellfish Immunology 89 (2019) 393–402

Contents lists available at ScienceDirect

Fish and Shellfish Immunology

journal homepage: www.elsevier.com/locate/fsi

Full length article

Dynamic distribution of formalin-inactivated *Edwardsiella tarda* in flounder (*Paralichthys olivaceus*) post intraperitoneal vaccination

Xiaoqian Tang[a,b], Jiaojiao Gong[a], Chuili Zeng[a], Xiuzhen Sheng[a], Jing Xing[a,b], Wenbin Zhan[a,b,*]

[a] Laboratory of Pathology and Immunology of Aquatic Animals, KLMME, Ocean University of China, 5 Yushan Road, Qingdao, 266003, China
[b] Laboratory for Marine Fisheries Science and Food Production Processes, Qingdao National Laboratory for Marine Science and Technology, Qingdao, 266071, China

ARTICLE INFO

Keywords:
Flounder (*Paralichthys olivaceus*)
Edwardsiella tarda
Intraperitoneal injection
Antigen uptake

ABSTRACT

In order to investigate the dynamic distribution of antigen in different tissues post vaccination, an absolute real-time quantitative PCR was employed to detect the amount of antigen in flounder (*Paralichthys olivaceus*) post intraperitoneal (i.p.) injection with three concentrations (10^7, 10^8, 10^9 CFU ml^{-1}) of formalin-inactivated *Edwardsiella tarda* bacterin. The results showed that the amount of uptaken antigen quickly increased and then decreased in different tissues. The peak occurred first in the spleen and head kidney at 6–9 h after injection, and in the liver and blood at 9–15 h, then in the gill, intestine and skin at 15–24 h, finally in the muscle at 24–36 h. The amount of antigen was highest in the spleen and head kidney, followed by the blood, liver and gill, and lowest in the intestine, skin and muscle. Among the three concentration groups, the amount of antigen increased with the increasing concentration of the vaccine in the blood, liver, gill, intestine, skin and muscle, except for the spleen and head kidney, in which more antigens were found in the 10^8 CFU ml^{-1} group than that in 10^9 CFU ml^{-1} group. Moreover, IIFA and western blotting was performed to examine the tissue distribution of antigen at 9 h after vaccination with 10^8 CFU ml^{-1} formalin-inactivated *E. tarda*. The bacteria were mainly observed in the spleen and head kidney, then the liver, gill and blood, and least in the intestine, skin and muscle, which was roughly in accordance with the results of absolute qPCR. Furthermore, the expressions of CD4-1, MHC IIα, CD8α and MHC Iα in different tissues were detected by RT-qPCR, and the expression levels of these genes were highest in the spleen and head kidney, then in the blood, gill, liver, and lowest in the intestine, skin and muscle. All these results provided useful information for dynamic transportation of antigen uptake post vaccination, and also deepened the understanding of immune response to the injection vaccination.

1. Introduction

Edwardsiella tarda is a Gram-negative bacterium, causing edwardsiellosis in freshwater and marine fish, which has resulted in extensive economic losses to aquaculture industry [1]. Currently, vaccines are considered as the economic, environmental friendly and safety strategy to prevent the outbreak of edwardsiellosis in aquaculture, and various types of *E. tarda* vaccines have been developed including recombinantly attenuated vaccine, genetic vaccine, natural avirulent strain vaccine, formalin-killed vaccine and ghost bacteria vaccine [2–6]. The formalin-killed *E. tarda* was reported to be a traditional and economic vaccine, not only for the reason that it can elicit protective immune response, but also for the diversity of delivery methods, including injection, immersion or oral vaccination [7–9]. The intraperitoneal (i.p.) vaccination is the most common used method in aquaculture, which ensures that a certain amount of vaccine could be inoculated and induces an effective and durable immune-protection for fish against pathogen infections [10]. However, the research on the dynamic change of antigen uptake in different tissues *in vivo* post intraperitoneal injection vaccination was still lacking.

Several factors have been shown to influence the uptake of antigens such as vaccine dose, the type of immunogen, the effectiveness of immunization strategies and the use of adjuvant [11,12]. The amount of antigen taken up by lymph tissues will affect the vaccination efficacy, which could be an indicator for evaluating the effect of injection vaccination [13,14]. Although, the property of immunogen is considered as the most influential factor for the immune efficiency of the vaccine, there is still a certain relationship between the efficacy and the vaccine dose within a certain range of dose. It was reported that a higher amount of formalin-inactivated *E. tarda* uptaken by immune-related

* Corresponding author. Laboratory of Pathology and Immunology of Aquatic Animals, KLMME, Ocean University of China, 5 Yushan Road, Qingdao, 266003, China.
E-mail address: wbzhan@ouc.edu.cn (W. Zhan).

https://doi.org/10.1016/j.fsi.2019.04.022
Received 4 December 2018; Received in revised form 5 April 2019; Accepted 8 April 2019
Available online 11 April 2019

tissues could trigger a stronger immune response after immersion vaccination [15,16]. Therefore, the study of the dynamic distribution of vaccinated antigen will contribute to the understanding of the antigen uptake mechanism and the optimization of vaccination strategies [17,18]. In the recent years, different types of antigens were employed to investigate the antigen presentation, including lipopolysaccaride (LPS) and protein of bacteria, inactivated or live bacteria, alum-precipitated bovine serum albumin (AP-BSA), fluorescein conjugation with bacterin and inactivated virus [19–23]. Till now, several methods were developed for detecting the antigen uptake, such as absolute quantitative PCR (qPCR), plate culture, electron microscopy, immunohistochemistry, *in situ* hybridization or optical projection tomography (OPT) [18,19,24]. Among them, absolute qPCR provides a more convenient and sensitive way to measure the amount of antigen uptake and avoid complicated and time-consuming procedures [25]. Our previous work illustrated the influence of concentration of bacterin, immersion time and hyperosmotic treatment on the antigen uptake, and the process of antigen uptake was detected within a short time [16,17]. However, the information about the process of antigen uptake in different immune-related tissues after i.p. injection with different concentration vaccine was still lacking.

In the present study, absolute qPCR was developed to investigate the dynamic change of antigen uptake in the eight main tissues of flounder after i.p. injection with three concentrations (10^7, 10^8, 10^9 CFU ml^{-1}) of formalin-inactivated *E. tarda* vaccine. Moreover, indirect immunofluorescence assay (IIFA) and wester blotting were used to examine the distribution of antigen in flounder. Furthermore, a reverse transcription quantitative PCR (RT-qPCR) was developed to investigate the expression level of major histocompatibility complex class Iα and IIα (MHC Iα and MHC IIα) and T cell surface receptors (CD4-1 and CD8α).

2. Materials and methods

2.1. The experimental fish

Healthy flounders (*Paralichthys olivaceus*) (average length: 15–17 cm) were obtained from a fish farm of Rizhao City, Shandong province, China. The fish were quarantined in the laboratory condition (temperature 20 ± 1 °C, dissolved oxygen concentration 6.5 ± 0.5 mg L^{-1}, water salinity 28 ± 1%), and fed with dry commercial diet every day.

2.2. Preparation of inactivated E. tarda bacterin and rabbit polyclonal antibodies

The strain of *E. tarda* HC01090721 was originally isolated from the ascites of flounder and stored in saline with 15% glycerol at −80 °C, and prepared as previous describe [26]. Briefly, the bacteria were grown on brain heart infusion (BHI) agar plate at 37 °C for 48 h, and then single clones were selected and transferred into BHI-broth and incubated at 37 °C. After reaching the stationary phase (OD_{600} = 1.0), the bacteria were harvested and washed with 0.01 M phosphate-buffered saline (PBS, pH 7.2) and treated with 0.5% formalin (V/V) for 96 h at 4 °C. The safety of the inactivated *E. tarda* was checked by culturing the cells on BHI agar for 3 days at 37 °C. The inactivated cells were harvested and washed 3 times with sterilized PBS by centrifuging at 8000 × *g* for 10 min. After the last wash, the concentration of bacteria was adjusted to 1.0 × 10^{10} CFU ml^{-1} for later use.

The formalin-inactivated *E. tarda* was used as immunogen to prepare the rabbit *anti-E. tarda* polyclonal antisera as described previously [27]. The rabbit was immunized four times, and when the titer reached to 1:20,000–50,000, the polyclonal antiserum was taken by drawing blood from heart under anesthesia. Rabbit IgG was purified using protein G-agarose fast flow column (Sigma) and characterized by enzyme-linked immunosorbent assay (ELISA), indirect immunofluorescence assay (IIFA) and flow cytometry (FCM).

For ELISA, 100 μl of *E. tarda* (5 × 10^7 CFU ml^{-1}) were coated on 96-well flat-bottom microplates (Costar, USA) and incubated overnight at 4 °C. Subsequently, the wells were washed thrice with PBS containing 0.05% Tween-20 (PBST) and then blocked with 200 μL 3% bovine serum albumin (BSA) in PBS for 1 h at 37 °C. After washing as above, wells were incubated with 100 μL *anti-E. tarda* polyclonal antibodies diluted at the ratios of 1:250, 1:500, 1:1000, 1:2000, 1:4000, 1:8000, 1:16000, 1:32000, 1:64000, 1:128000 with PBS for 1 h at 37 °C. Following PBST washes, 100 μL of AP-conjugated goat anti-rabbit IgG (Sigma, USA) diluted 1:1000 in PBS was added and incubated for 1 h at 37 °C. After the last washing, 100 μL 0.1% (w/v) *p*-nitrophenyl phosphate (pNPP, Sigma, USA) in pNPP buffer (1% diethanolamine, 0.5 mM MgCl2, pH 9.8) was added to each well and incubated for 30 min at room temperature (RT) in dark. The reaction was stopped with 50 μL per well of 2 M NaOH and absorbance was measured with an automatic ELISA reader at 405 nm (Molecular Devices, US). The serum of unimmunized rabbit was used as negative control. Each experiment was repeated in triplicate.

For IIFA, 100 μL of *E. tarda* solution was dropped on glass slides for 2 h sedimentation. Firstly, the bacteria were fixed with 4% paraformaldehyde for 15 min, then pre-incubated with 3% (w/v) BSA in PBS for 30 min to block non-specific antibody binding, and followed by an incubation with rabbit *anti-E. tarda* polyclonal antibodies (1:2000 dilution) at 37 °C for 90 min in a moisture chamber. For the negative control, normal rabbit serum (1:2000 dilution) was used. After washing three times with PBST, the *E. tarda* bacteria were incubated with Alexa Fluor 488-conjugated goat anti-rabbit IgG (1:1000) for 45 min at 37 °C. After three washes in PBST, the slides were observed under a fluorescence microscope (Olympus BX51). Meanwhile, the fluorescent staining of *E. tarda* with rabbit polyclonal antibodies was also performed in 1.5 ml Eppendorf tube, and then analyzed by Accuri C6 cytometer (BD AccuriTM, USA).

2.3. Vaccination and sampling

The flounders were randomly divided into four groups of 60 each, and each group were averagely subdivided into 3 tanks and immersed in an indoor temperature-controlled facility. The experimental groups were intraperitoneally injected with 200 μl of three concentrations (10^7, 10^8, 10^9 CFU ml^{-1}) of formalin-killed *E. tarda*, respectively, and the control group was intraperitoneally injected with same volume of PBS. Prior to sampling, the flounders were anesthetized with 300 ng ml^{-1} MS-222 (Sigma, USA) for 15 min. At 9 h post i.p. injection, 3 flounders were randomly sampled from the 10^8 CFU ml^{-1} group and control group. The intestine, skin, spleen, head kidney, liver, muscle and gill were collected and embedded in frozen section compound (Surgipath FSC22, Leica) and stored at −80 °C for IIFA and western blotting. At 0, 3, 9, 15, 24, 36, 48, 72 and 96 h post i.p. injection, 6 fish (2 fish from each tank) were randomly sampled from each group. Before dissection of the fish, blood samples were taken from the vena caudalis using heparinized syringes. Following wash three times with sterilized PBS to remove the adhesive antigen, the intestine, skin, spleen, head kidney, liver, muscle and gill were carefully taken separately and place into tubes containing 1 ml RNAlater® (Ambion, Austin, Texas). All the samples were independently collected and stored at −80 °C for RNA and DNA extraction. All the fish were anesthetized with MS-222 prior to sampling. The fish used in this study was carried out strictly in line with procedures in the Guide for the Use of Experimental Animals of Ocean University of China. In this study, the methods used in the animal experiments were approved by the Instructional Animal Care and Use Committee of the Ocean University of China (permit number: 20150101). All possible effort was dedicated to minimizing suffering.

2.4. Preparation of genomic DNA and cDNA

The genomic DNA of all sampled tissues was extracted using the DNeasy Blood & Tissue Kit (Qiagen, Germany) according to the manufacturer's protocol, and then measured and adjusted to 100 ng μl^{-1} using NanoDrop ND-8000 (Thermo Scientific, USA).

Total RNA was extracted from equal portions samples by Trizol (Sigma, USA) according to the manufacturer's instructions. The concentration of the RNA was detected by NanoDrop ND-8000 spectrophotometer, and the integrity of RNA was evaluated by 1.5% agarose gel. To ensure complete removal of genomic DNA (gDNA), 1 μg of total RNA was incubated with 1 unit of DNase I for 15 min at room temperature. Complementary DNA (cDNA) was synthesized by using Reverse Transcriptase M-MLV kit (TaKaRa, China) according to manufacturer's instructions and stored at −20 °C for RT-qPCR.

2.5. Detection of E. tarda in different tissues by absolute real-time qPCR

The absolute qPCR standard curve was established based on a previous research in our laboratory [17]. 2 μg DNA was extracted from 3.3×10^8 CFU ml^{-1} of *E. tarda* using DNeasy Blood & Tissue Kit (Qiagen, Germany) and diluted in 10-fold serial dilution series as templates to create the standard curve. The absolute qPCR assay was performed in triplicate for each dilution using Roche480 real-time PCR system (LightCycler480, USA). Reaction mixtures (20 μl) containing 10 μl of SYBR Green (Roche, Sweden), 0.4 μl each of forward and reverse primers, 7.2 μl of RNase-free water and 2 μl of *E. tarda* DNA. The standard cycling included an initial denaturation step at 95 °C for 5 min, followed by 45 cycles of denaturation at 94 °C for 30 s, annealing at 60 °C for 10 s and extension at 72 °C for 10 s. The standard curve equation $y = -3.515\ x + 43.78$ ($R^2 = 0.994$) was obtained base on the equation $y = a \times x + b$ (where y is Ct value and x is the logarithm of initial template quantity). The final values were converted to the amount of antigen in the 1 μg total DNA extracted from each tissue. The efficacy of the detected and specific amplicon was ensured by DNA melting-curve analysis, and the detection sensitivity of the absolute qPCR was determined based on the highest dilution that resulted in a detectable amplification signal.

2.6. E. tarda tissue distribution analysis by IIFA and western blotting

Continuous 6 μm thick frozen sections of tissues selected from 10^8 CFU ml^{-1} group and control group were cut using a Leica CM1900 cryostat at −20 °C and immersed with pre-cooled (4 °C) acetone for 15 min. Meanwhile, the whole blood cells settled on glass slides for 2 h, and fixed for 20 min at 22 °C with 4% paraformaldehyde. For IIFA, all the steps were performed as above. Briefly, the frozen sections and blood cell smears were washed with PBST for 5 min, then pre-incubated with 3% (w/v) BSA in PBS to block non-specific antibody binding, and followed by an incubation with rabbit *anti-E. tarda* polyclonal antibodies. The normal rabbit serum (1:2000 dilution) was used instead of antiserum as control. After washing three times, the sections were incubated with Alexa Fluor 488-conjugated goat anti-rabbit IgG (1:1000) containing 1 μg/ml Evans blue dye (EBD) (Fluka, Lyon, France) as the counterstain. All the sections were conducted at 37 °C for 45 min. Finally, the slides were observed under a fluorescence microscope (Olympus BX51).

For western blotting, total proteins of each tissue were extracted with RIPA Lysis buffer (Beyotime, China) according to the manufactures' instruction. The concentration of tissue proteins was analyzed with BCA kit (Beyotime, China), and adjusted it to 2 mg/mL. After SDS-PAGE, the proteins were transferred onto a PVDF membrane (Millipore, Germany). The membranes were blocked with PBS containing 5% bovine serum albumin (BSA) at 4 °C overnight, then washed three times with PBS. After that, the membrane was incubated with rabbit *anti-E. tarda* polyclonal antibody (1:2000) and HRP-goat-*anti*-rabbit IgG (1:5000, Beyotime, China) in turn. The immunoreactive bands were detected using enhanced chemiluminescence (ECL) technique. The main band of E. *tarda* that can be recognized by the antibody was used to represent the exist of bacteria in different tissues.

Table 1
Primers selected for Real time quantitative PCR analysis.

Primer name	Primer sequence(5′-3′)	Source
E. tarda 16S rDNA	F: TAGGGAGGAAGGTGTGAA R: CTCTAGCTTGCCAGTCTT	CP001135.1
EF1α	F: CTCCACTGAGCCCCCTTACA R: GTCTCCGTGCCAACCAGAGA	AB017183
CD4-1	F:CCAGTGGTCCCCACCTAAAA R:CACTTCTGGGACGGTGAGATG	AB643634
CD8α	F: ATTAGTTGTGAAAGAGGGGGC R: TGAGGAATCAATGTATGGGGA	AB082957
MHCIα	F: AGACCACAGGCTGTTATCACCA R: TCTTCCCATGCTCCACGAA	AB126921
MHCIIα	F: ACAGGGACGGAACTTATCAACG R: TCATCGGACTGGAGGGAGG	AY997530

2.7. Expression analysis of four antigen presentation-related genes by RT-qPCR

The expression profiles of four antigen presentation-related immune genes including MHC Iα、MHC IIα、CD4-1 and CD8α were detected by RT-qPCR with specific primers (shown in Table 1). The cDNA concentrations of each tissue was diluted 10-fold as template for RT-qPCR. Each reaction well contained 10 μl of SYBR Green I Master, 0.4 μl each of forward and reverse primers, 2 μl of diluted cDNA and 7.2 μl of RNase-free water to a total volume of 20 μl. The thermal cycling profile consisted of an initial denaturation at 95 °C for 30 s, followed by 45 cycles of denaturation at 95 °C for 5 s and extension at 60 °C for 30 s. Each assay was performed in triplicate with EF1α gene as the endogenous control. All data were analyzed relative to the EF1α gene by the $2^{-\Delta\Delta Ct}$ method [28].

2.8. Statistical analysis

Data were presented as arithmetic mean values. Statistical analysis was performed by SPSS software (Version 20.0; SPSS, IBM, Armonk, NY, USA) and the differences were analyzed by variance (ANOVA) and Duncan's multiple comparison test. The statistical software origin 8.0 was used for creating graphs.

3. Results

3.1. Quantification of E. tarda antigen in different tissues

Absolute qPCR assay targeting the 16S rDNA gene was employed to determine the changes of antigen amount in all sampled tissues of flounder post i.p. injection, and the data was shown in Fig. 1. In the control group, there was no *E. tarda* detected in the tissues (data not shown). In contrast, the amount of antigen in all sampled tissues of three concentration groups gradually increased and reached their peak levels at different times, and then underwent a decline. The amount of antigen reached the peak value in the spleen and head kidney at 6–9 h post i.p. injection (Fig. 1C and D), and in the blood and liver at 9–15 h (Fig. 1H and E), then in the gill, intestine and skin at 15–24 h (Fig. 1G, A and B), and finally in the muscle at 24–36 h (Fig. 1F). Moreover, among the three vaccination concentration groups, the antigen in different tissues had a similar distribution feature that the antigen number was highest in the spleen and head kidney, followed by in the blood, liver and gill, and lowest in the intestine, skin and muscle. The highest number of *E. tarda* reaching 1.3×10^4 CFU μg^{-1} DNA were observed in the head kidney in the 10^8 CFU ml^{-1} group, while the lowest value

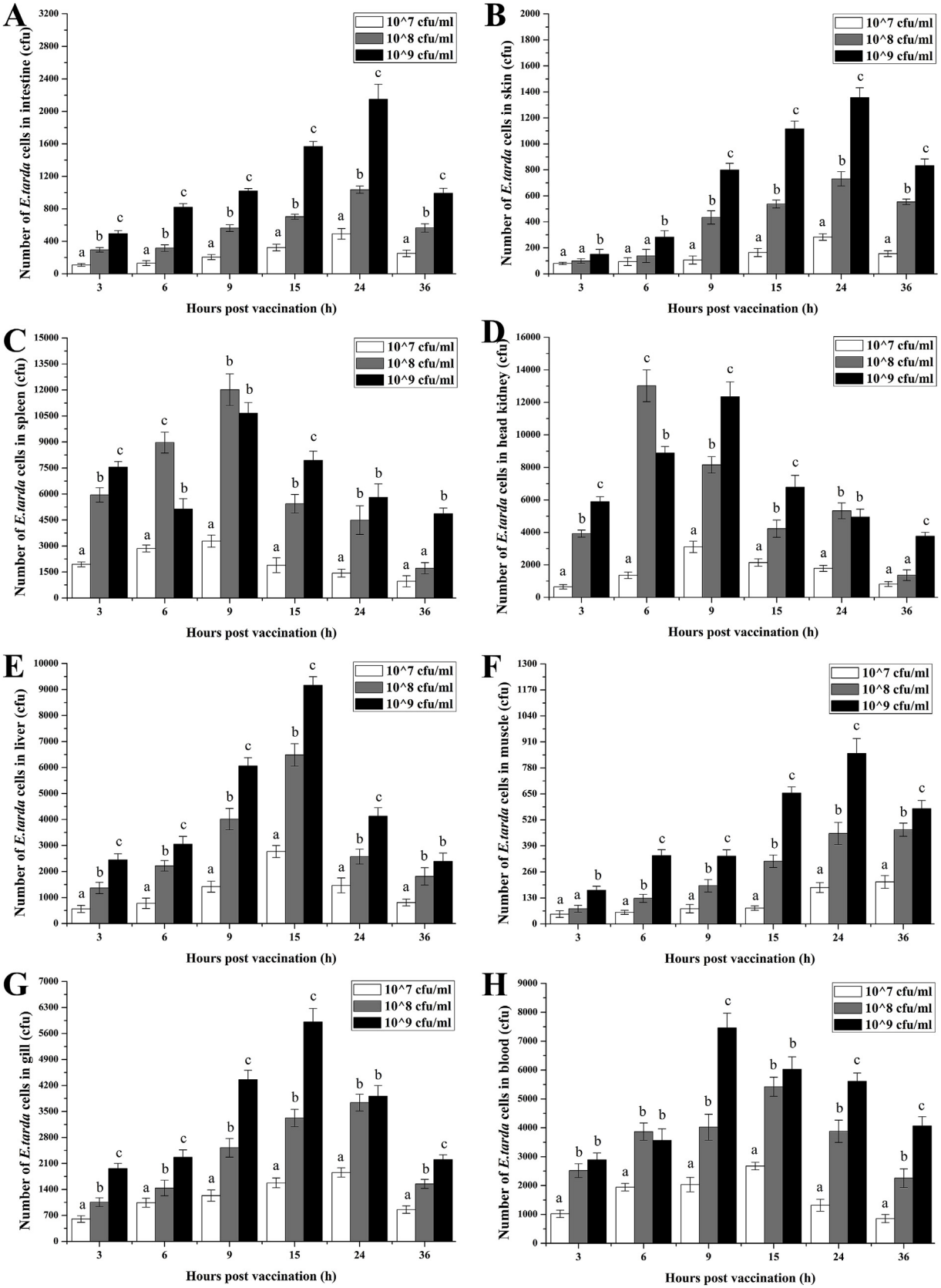

Fig. 1. The amount of inactivated *E. tarda* cells in the different tissues of flounder post i.p. injection. A. Intestine; B. Skin; C. Spleen; D. Head kidney; E. Liver; F. Muscle; G. Gill; H. Blood. Values were means ± SE of three replicates, and different letters denoted significant difference among groups at the same time ($P < 0.05$).

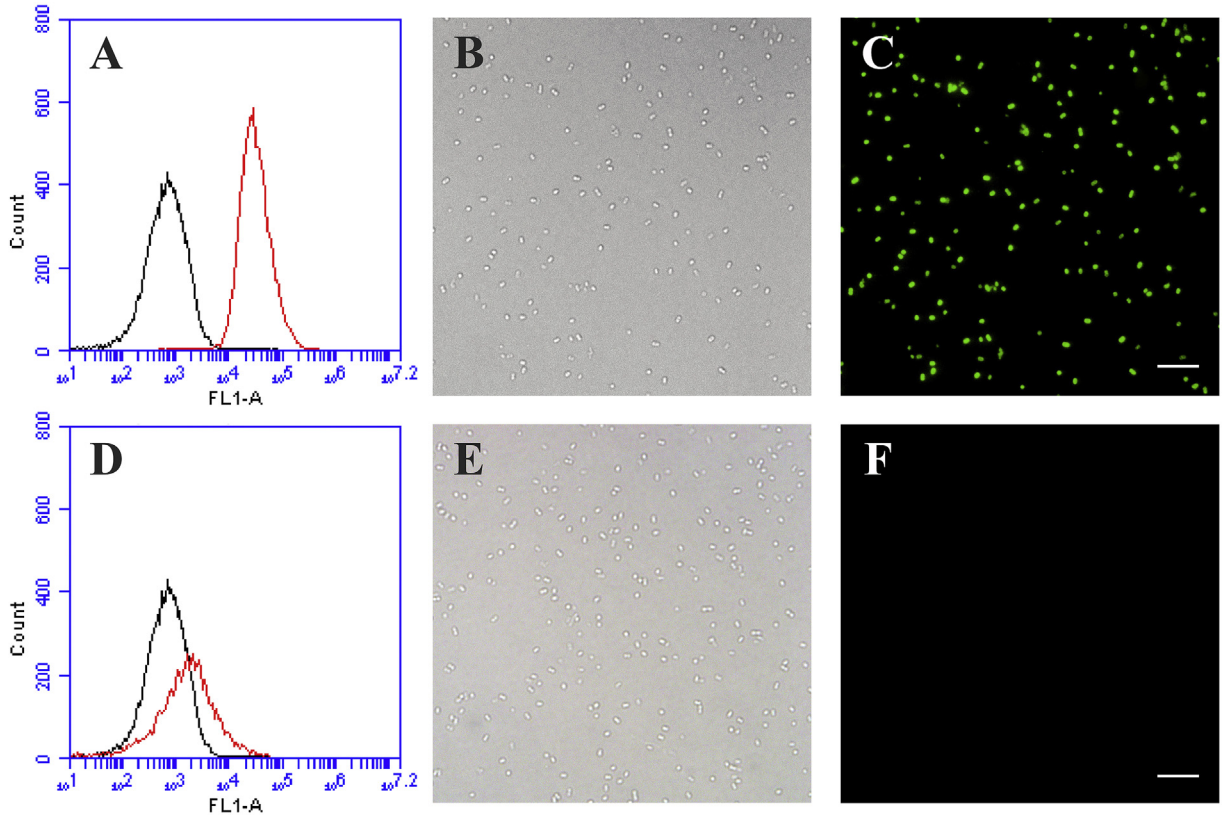

Fig. 2. The characteristic analysis of rabbit *anti-E. tarda* polyclonal antibodies. A. FCM result of *E. tarda* incubated with rabbit *anti-E. tarda* polyclonal antibodies (red peak), the black peak is blank control; B. *E. tarda* stained with the rabbit *anti-E. tarda* polyclonal antibodies; C. *E. tarda* were observed under the DIC microscope in the same field as shown in B. D. FCM result of *E. tarda* incubated with healthy rabbit serum (red peak), the black peak is blank control; E. *E. tarda* stained with healthy rabbit serum; F. The DIC microscope in the same field as shown in E. Bar = 10 μm. (For interpretation of the references to color in this figure legend, the reader is referred to the Web version of this article.)

approximately 50 CFU μg^{-1} DNA were detected in the muscle in the 10^7 CFU ml^{-1} group. Furthermore, the amount of antigen in different sampled tissues became higher with the increasing of vaccination concentration except for the spleen and head kidney, in which more antigen was found in the 10^8 CFU ml^{-1} group than that in the 10^9 CFU ml^{-1} group and 10^7 CFU ml^{-1} group.

3.2. Characteristics of rabbit anti-E. tarda polyclonal antibodies

The result of ELISA showed that the rabbit *anti-E. tarda* polyclonal antibodies diluted 1:64000 still showed positive (P/N = 2.4) and the highest OD value was observed in the dilution of 1:2000, which was used in the following experiments. The results of FCM and IIFA both showed that the *E. tarda* cells could be specifically recognized by the polyclonal antibodies (Fig. 2).

3.3. E. tarda tissue distribution analysis

According to the results of absolute real-time qPCR, we found that the amount of antigen reached a higher level for most detected tissues at 9 h post i.p. injection in the 10^8 CFU ml^{-1} group. Therefore, in order to clearly observe the presence of antigen in different tissues, we sampled the tissues at 9 h after i.p. injection for the indirect immunofluorescence assay and western blotting. The green fluorescence signal indicated positive signals of *E. tarda.* It can be seen clearly in the Fig. 3 that the uptake of *E. tarda* was observed in all tested tissues, while no green fluorescence signal was observed in the tissues sampled from control group. Among all detected tissues, the positive signals of antigen uptake were mainly localized in the spleen and head kidney (Fig. 3C and D), fewer in the liver, gill and blood (Fig. 3E, G and H), and fewest in the muscle, intestine and skin (Fig. 3F, A and B). Moreover, the result of western blotting also showed that spleen and head kidney were the primary organs to uptake the antigens (Fig. 4). These differences between tissues were roughly in line with the results of absolute qPCR. In addition, we also found that the bacteria distributed in different tissues were not all uptaken by phagocytic cells, some of them were trapped in tissue spaces (Fig. 3).

3.4. RT-qPCR analysis of four antigen presentation-related immune genes

RT-qPCR was performed to further evaluate the expression levels of antigen presentation-related immune genes including MHC Iα, MHC IIα, CD4-1 and CD8α in different tissues after i.p. injection. Compared to the blank control group, the mRNA levels of all detected genes in all sampled tissues gradually increased and reached their peak levels at different time points after vaccination, and then descended slowly (Figs. 5 and 6). The expression of MHC Iα and CD8α genes reached their peaks firstly in the spleen and head kidney at 24 h after i.p. injection, and followed by in the liver, gill and blood at 36 h, then in the intestine at 48 h, and finally in the skin and muscle at 72 h. The expression of MHC IIα and CD4-1 genes reached peak firstly in the spleen and head kidney at 36 h, then in the liver, gill and blood at 48 h, and finally in the intestine, skin and muscle at 72–96 h. Moreover, among three concentration groups, the expression of these four genes in the sampled tissues became higher with the increasing of vaccine concentration except for the spleen and head kidney. The expression levels of the four genes in the spleen and head kidney in the 10^9 CFU ml^{-1} group were much higher than that in the 10^7 CFU ml^{-1} group but lower than that in the 10^8 CFU ml^{-1} group.

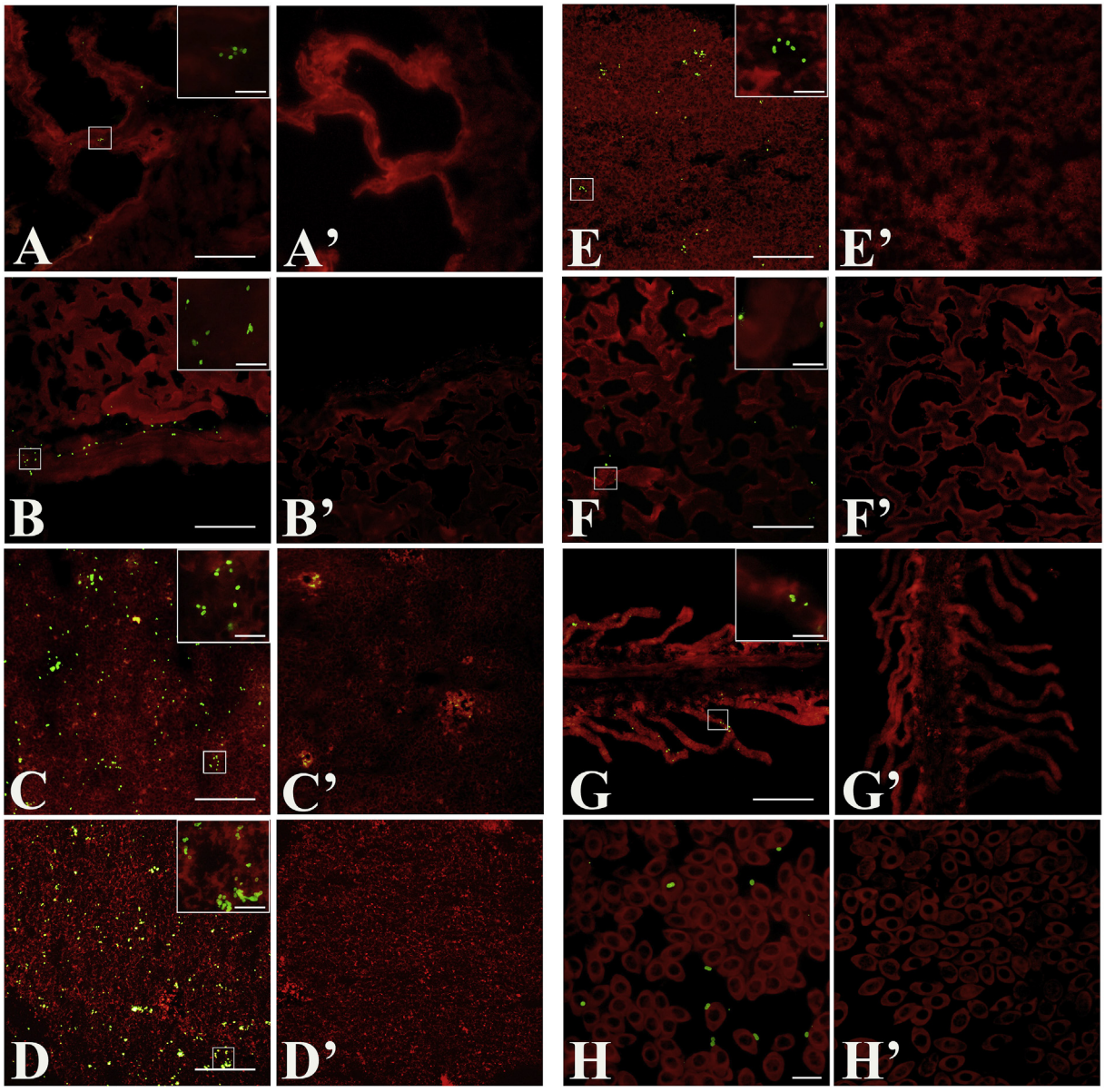

Fig. 3. Tissue distribution of *E. tarda* cells in flounder detected by IIFA at 9 h post vaccination with 10^8 CFU ml^{-1} formalin-killed *E. tarda*. The green fluorescence (arrow) indicated positive signals of *E. tarda*. A. Intestine; B. Skin; C. Spleen; D. Head kidney; E. Liver; F. Muscle; G. Gill; H. Blood. (A–G) Bar = 100 μm; (H) Bar = 10 μm. The corresponding enlarged drawing was shown in the upper right of the picture. Bar = 10 μm. No green signal was present in the control group (A′-H′). Experimental group (A–H) and control group (A′-H′) were incubated with rabbit *anti-E. tarda* polyclonal antibodies and Alexa Fluor 488-conjugated goat anti-rabbit IgG. All tissues were stained in red by EBD. (For interpretation of the references to color in this figure legend, the reader is referred to the Web version of this article.)

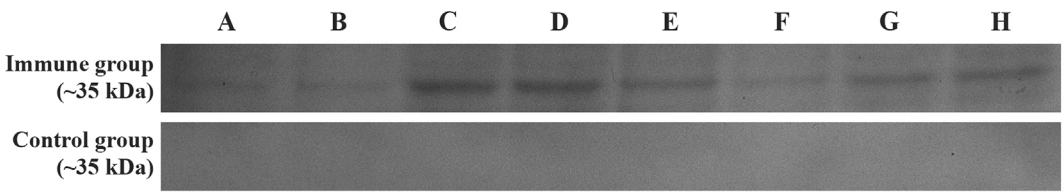

Fig. 4. Tissue distribution of *E. tarda* cells in flounder detected by western blotting at 9 h post vaccination with 10^8 CFU ml^{-1} formalin-killed *E. tarda*. A. Intestine; B. Skin; C. Spleen; D. Head kidney; E. Liver; F. Muscle; G. Gill; H. Blood.

4. Discussion

In mammals, the lymphatic absorption and drainage routes of the peritoneal cavity have been widely studied, which could form a specialized system transporting fluid from the peritoneal cavity to the blood circulation system [29,30]. It has been reported in rats that the intraperitoneally injected liposomes-vesicles are transported from the peritoneal activity to the blood and are subsequently taken up mainly by liver and spleen [31]. In teleost fish, there is lack of diaphragm and lymph nodes, however, several studies reported that some antigens like

A

Fold changes in the intestine	Genes	Groups	0h		3h		9h		15h		24h		36h		48h		72h		96h	
			Fold	SEM	Fold	SEM	Fold	SEM	Fold	SEM	Fold	SEM	Fold	SEM	Fold	SEM	Fold	SEM	Fold	SEM
	CD4-1	10^7	1.00	0.16	0.91	0.13	1.09	0.09	1.52	0.08	1.65	0.20	1.77	0.28	1.63	0.13	1.89	0.34	1.74	0.33
		10^8	1.00	0.29	0.74	0.08	1.03	0.68	1.10	0.10	1.89	0.18	1.97	0.08	2.72	0.28	3.17	0.31	1.03	0.30
		10^9	1.00	0.14	1.41	0.32	0.89	0.23	1.22	0.20	2.54	0.26	3.00	0.19	4.29	0.19	7.23	0.16	2.07	0.21
	MHCIIα	10^7	1.00	0.10	1.32	0.34	1.08	0.19	1.28	0.25	1.27	0.24	1.51	0.37	2.78	0.15	3.48	0.35	1.35	0.23
		10^8	1.00	0.36	1.35	0.16	1.05	0.11	1.17	0.21	1.55	0.27	1.71	0.09	3.01	0.31	3.32	0.04	2.09	0.22
		10^9	1.00	0.24	2.51	0.15	2.22	0.32	1.74	0.11	1.71	0.19	2.36	0.11	4.78	0.21	4.99	0.43	0.87	0.30
	CD8α	10^7	1.00	0.38	1.21	0.43	1.10	0.30	1.08	0.38	1.81	0.06	1.73	0.11	2.19	0.19	2.07	0.12	1.61	0.20
		10^8	1.00	0.16	1.01	0.14	1.27	0.07	1.05	0.03	1.84	0.19	2.12	0.11	2.49	0.28	2.26	0.08	1.39	0.21
		10^9	1.00	0.22	2.18	0.33	2.35	0.29	2.97	0.08	3.56	0.12	3.71	0.13	6.31	0.20	5.92	0.06	1.62	0.40
	MHCIα	10^7	1.00	0.27	1.46	0.31	1.26	0.08	1.51	0.35	2.08	0.18	2.28	0.21	3.48	0.28	2.17	0.27	1.75	0.32
		10^8	1.00	0.17	0.95	0.13	1.23	0.09	0.91	0.06	1.39	0.23	2.05	0.06	3.34	0.37	1.61	0.19	1.20	0.27
		10^9	1.00	0.10	2.43	0.35	2.31	0.31	1.69	0.25	2.35	0.16	3.66	0.37	5.97	0.14	3.51	0.18	1.17	1.05

B

Fold changes in the skin	Genes	Groups	0h		3h		9h		15h		24h		36h		48h		72h		96h	
			Fold	SEM	Fold	SEM	Fold	SEM	Fold	SEM	Fold	SEM	Fold	SEM	Fold	SEM	Fold	SEM	Fold	SEM
	CD4-1	10^7	1.00	0.16	1.32	0.12	1.54	0.21	1.61	0.12	1.65	0.17	1.67	0.31	1.82	0.17	1.89	0.32	2.53	0.23
		10^8	1.00	0.10	1.49	0.16	1.69	0.06	1.71	0.03	1.59	0.45	1.53	0.13	2.06	0.27	2.80	0.14	3.66	0.13
		10^9	1.00	0.14	1.01	0.43	1.05	0.20	0.81	0.24	1.10	0.63	1.62	0.14	2.56	0.19	4.32	0.16	4.56	0.06
	MHCIIα	10^7	1.00	0.45	1.04	0.16	1.25	0.27	1.56	0.07	2.23	0.37	2.55	0.41	3.12	0.23	3.32	0.16	3.45	0.24
		10^8	1.00	0.21	1.00	0.15	1.34	0.13	1.40	0.12	1.24	0.15	1.12	0.10	1.79	0.15	2.08	0.17	2.48	0.27
		10^9	1.00	0.22	1.21	0.20	1.15	0.29	1.35	0.28	1.87	0.27	1.63	0.13	2.80	0.08	4.87	0.16	5.21	0.27
	CD8α	10^7	1.00	0.28	0.98	0.25	0.90	0.30	1.15	0.17	1.36	0.19	1.71	0.10	1.94	0.10	2.31	0.28	1.48	0.24
		10^8	1.00	0.26	1.07	0.15	1.22	0.36	1.41	0.06	1.53	0.28	1.76	0.13	1.92	0.15	2.10	0.16	1.38	0.27
		10^9	1.00	0.41	1.81	0.22	1.18	0.17	1.51	0.12	2.09	0.34	2.33	0.15	3.78	0.19	5.36	0.21	1.67	0.13
	MHCIα	10^7	1.00	0.52	1.13	0.16	1.39	0.17	1.59	0.23	2.42	0.17	2.58	0.28	2.85	0.18	3.00	0.09	1.97	0.39
		10^8	1.00	0.22	1.37	0.06	1.13	0.32	0.96	0.06	1.72	0.32	1.74	0.36	2.03	0.17	3.27	0.22	1.55	0.39
		10^9	1.00	0.18	1.16	0.19	1.92	0.18	1.86	0.23	1.88	0.21	2.84	0.25	4.15	0.15	7.18	0.20	1.19	0.15

C

Fold changes in the spleen	Genes	Groups	0h		3h		9h		15h		24h		36h		48h		72h		96h	
			Fold	SEM	Fold	SEM	Fold	SEM	Fold	SEM	Fold	SEM	Fold	SEM	Fold	SEM	Fold	SEM	Fold	SEM
	CD4-1	10^7	1.00	0.32	2.60	0.22	2.70	0.29	4.30	0.21	6.60	0.11	15.58	0.22	15.56	0.24	9.83	0.49	5.54	0.15
		10^8	1.00	0.26	6.73	0.23	7.87	0.21	11.13	0.09	16.37	0.07	27.27	0.14	17.88	0.20	10.48	0.08	4.44	0.20
		10^9	1.00	0.30	9.36	0.36	10.58	0.16	17.23	0.06	15.63	0.30	26.34	0.21	16.16	0.29	14.42	0.07	8.33	0.26
	MHCIIα	10^7	1.00	0.28	3.74	0.36	5.10	0.31	4.28	0.06	4.94	0.21	11.52	0.35	11.18	0.14	8.65	0.13	3.87	0.39
		10^8	1.00	0.28	4.95	0.10	6.32	0.21	4.87	0.20	10.03	0.12	25.51	0.17	14.55	0.14	7.33	0.10	2.45	0.50
		10^9	1.00	0.28	6.63	0.26	5.58	0.03	8.46	0.19	8.34	0.30	20.90	0.42	17.88	0.31	8.65	0.29	3.97	0.30
	CD8α	10^7	1.00	0.25	2.74	0.56	3.60	0.08	4.01	0.26	17.36	0.30	14.19	0.32	7.28	0.20	5.18	0.39	2.74	0.34
		10^8	1.00	0.27	7.57	0.09	9.99	0.55	9.34	0.20	31.00	0.07	21.63	0.16	10.88	0.17	5.66	0.04	3.47	0.11
		10^9	1.00	0.20	8.53	0.38	12.50	0.21	11.42	0.18	23.93	0.15	21.41	0.04	7.73	0.03	6.63	0.06	8.51	0.17
	MHCIα	10^7	1.00	0.33	2.68	0.22	2.65	0.36	5.43	0.23	12.84	0.24	6.61	0.30	7.38	0.22	5.35	0.25	3.15	0.21
		10^8	1.00	0.57	4.07	0.07	7.45	0.13	9.43	0.14	33.99	0.08	23.28	0.51	6.35	0.18	3.78	0.19	2.05	0.10
		10^9	1.00	0.19	3.46	0.25	8.21	0.11	14.49	0.11	22.25	0.18	13.70	0.21	8.67	0.11	4.77	0.21	2.02	0.25

D

Fold changes in the head kidney	Genes	Groups	0h		3h		9h		15h		24h		36h		48h		72h		96h	
			Fold	SEM	Fold	SEM	Fold	SEM	Fold	SEM	Fold	SEM	Fold	SEM	Fold	SEM	Fold	SEM		SEM
	CD4-1	10^7	1.00	0.26	3.93	0.06	4.82	0.02	5.03	0.31	6.09	0.22	10.95	0.04	10.35	0.23	9.32	0.16	5.82	0.14
		10^8	1.00	0.11	5.22	0.49	8.65	0.46	10.10	0.21	12.30	0.41	30.59	0.29	23.75	0.31	10.00	0.37	4.72	0.15
		10^9	1.00	0.15	6.11	0.21	9.19	0.14	10.93	0.07	12.61	0.05	26.22	0.15	20.11	0.03	9.40	0.15	2.75	0.10
	MHCIIα	10^7	1.00	0.36	3.14	0.34	4.00	0.19	4.99	0.25	4.91	0.34	8.21	0.28	13.39	0.08	7.24	0.37	3.21	0.30
		10^8	1.00	0.12	6.90	0.15	7.14	0.23	7.08	0.15	17.31	0.09	31.27	0.20	14.55	0.27	11.08	0.09	4.97	0.28
		10^9	1.00	0.12	4.40	0.14	6.85	0.22	10.78	0.36	16.60	0.25	17.43	0.18	13.44	0.12	11.66	0.24	7.28	0.27
	CD8α	10^7	1.00	0.29	4.73	0.17	5.11	0.28	6.41	0.06	14.48	0.29	13.61	0.26	7.18	0.20	5.67	0.16	3.78	0.24
		10^8	1.00	0.19	2.50	0.18	3.52	0.06	4.39	0.16	33.28	0.35	22.52	0.06	15.28	0.25	10.88	0.26	7.48	0.17
		10^9	1.00	0.22	9.08	0.17	13.45	0.26	16.04	0.06	21.04	0.09	15.99	0.07	20.11	0.09	12.50	0.13	3.88	0.48
	MHCIα	10^7	1.00	0.30	2.90	0.23	2.66	0.02	6.41	0.76	8.75	0.10	7.12	0.11	7.43	0.17	6.42	0.17	3.61	0.32
		10^8	1.00	0.11	2.26	0.10	7.66	0.15	10.85	0.13	32.52	0.26	19.34	0.04	9.30	0.42	3.55	0.14	1.89	0.10
		10^9	1.00	0.35	7.00	0.16	6.22	0.38	12.44	0.09	27.39	0.02	25.75	0.17	12.01	0.30	7.24	0.26	2.87	0.36

Fig. 5. Relative expression of CD4-1, MHC IIα, CD8α and MHC Iα genes in the different tissues of flounder. A. Intestine; B. Skin; C. Spleen; D. Head kidney. The data are presented as the means ± SEM and the length of the color bars indicate the extent of upregulated expressions of the genes. (For interpretation of the references to color in this figure legend, the reader is referred to the Web version of this article.)

vitellogenin and colloidal carbon could be readily transported from the peritoneal cavity into the blood and then transported into other lymphoid tissues with blood circulation [32,33]. In the present study, the amount of antigen in the blood reached peak level at an early time post vaccination, and then the antigen in the liver, gill, intestine, skin and muscle gradually increased, which indicated that the injected antigen in intraperitoneal cavity was firstly transported into blood circulation and then intercepted by the liver, gill, intestine, skin and muscle. These results indicated that there might be a mechanism in which the antigen could be transported from the abdominal cavity into the blood circulation and eventually into other tissues. To be noted, the amount of antigen reached peak earlier in the spleen and head kidney than that in the blood, which suggested that the spleen and head kidney might have an extensive capacity to uptake the antigen from blood circulation and could intercepted a large amount of antigen in a short time.

The intake of antigen varies greatly in different tissues, and the amount of antigen was highest in the spleen and head kidney, followed by in the blood, liver and gill, and lowest in the intestine, skin and muscle. As is known, both spleen and head kidney are antigen-trapping organs to possess populations of macrophages and lymphocytes which facilitate antigen retrieval, trap substances and particles antigen [34]. The melanomacrophage centres of spleen and head kidney are able to

A — Fold changes in the liver

Genes	Groups	0h Fold	0h SEM	3h Fold	3h SEM	9h Fold	9h SEM	15h Fold	15h SEM	24h Fold	24h SEM	36h Fold	36h SEM	48h Fold	48h SEM	72h Fold	72h SEM	96h Fold	96h SEM
CD4-1	10^7	1.00	0.19	3.97	0.10	4.42	0.03	5.87	0.17	5.76	0.20	9.08	0.26	14.42	0.12	6.01	0.06	3.51	0.24
	10^8	1.00	0.11	3.40	0.30	6.96	0.17	5.82	0.16	9.11	0.25	11.52	0.20	13.06	0.26	9.23	0.51	4.07	0.16
	10^9	1.00	1.05	3.73	0.09	5.43	0.60	9.49	0.17	9.71	0.26	11.06	0.35	20.58	0.35	15.45	0.34	9.34	0.53
MHCIIα	10^7	1.00	0.37	3.01	0.28	3.80	0.27	4.96	0.22	5.54	0.18	9.34	0.33	12.91	0.32	7.80	0.08	2.26	0.15
	10^8	1.00	0.12	5.66	0.27	6.68	0.28	8.48	0.12	11.21	0.08	14.42	0.14	18.55	0.25	8.53	0.20	5.50	0.27
	10^9	1.00	0.12	3.68	0.12	5.79	0.50	12.24	0.18	11.06	0.27	15.03	0.14	20.49	0.37	7.31	0.27	5.95	0.07
CD8α	10^7	1.00	0.36	4.03	0.22	4.11	0.32	5.40	0.24	7.06	0.29	15.45	0.19	12.88	0.23	9.25	0.22	4.09	0.32
	10^8	1.00	0.27	5.13	0.28	5.34	0.08	10.93	0.22	14.29	0.17	19.12	0.19	11.13	0.55	7.29	0.24	2.85	0.21
	10^9	1.00	0.05	8.38	0.15	9.21	0.59	7.80	0.27	17.47	0.46	24.31	0.40	18.59	0.40	8.36	0.24	5.64	0.10
MHCIα	10^7	1.00	0.16	3.42	0.01	3.61	0.37	4.67	0.25	6.25	0.41	12.97	0.32	9.67	0.30	7.09	0.32	4.00	0.13
	10^8	1.00	0.30	4.56	0.14	3.62	0.09	4.80	0.10	14.96	0.11	21.91	0.37	12.55	0.13	6.98	0.48	4.97	0.33
	10^9	1.00	0.33	4.86	0.12	7.08	0.42	6.60	0.32	14.19	0.31	24.08	0.27	14.52	0.13	8.40	0.43	2.65	0.28

B — Fold changes in the muscle

Genes	Groups	0h Fold	0h SEM	3h Fold	3h SEM	9h Fold	9h SEM	15h Fold	15h SEM	24h Fold	24h SEM	36h Fold	36h SEM	48h Fold	48h SEM	72h Fold	72h SEM	96h Fold	96h SEM
CD4-1	10^7	1.00	0.29	0.95	0.42	1.20	0.20	1.27	0.13	1.51	0.08	1.61	0.15	1.79	0.21	1.66	0.37	2.04	0.24
	10^8	1.00	0.24	1.28	0.10	1.27	0.42	1.58	0.37	1.38	0.23	1.87	0.05	2.15	0.30	2.13	0.19	2.23	0.17
	10^9	1.00	0.25	1.15	0.38	0.96	0.42	0.89	0.29	1.09	0.32	1.52	0.29	4.29	0.21	4.49	0.21	4.52	1.21
MHCIIα	10^7	1.00	0.30	1.38	0.28	1.33	0.35	1.54	0.45	1.56	0.37	1.80	0.39	2.17	0.14	2.07	0.17	2.66	0.45
	10^8	1.00	0.24	1.49	0.07	1.31	0.28	1.52	0.09	1.64	0.26	1.47	0.14	2.03	0.10	3.09	0.09	3.19	0.21
	10^9	1.00	0.25	1.20	0.10	1.97	0.43	1.96	0.28	2.17	0.25	3.03	0.39	3.87	0.33	4.04	0.45	4.91	0.15
CD8α	10^7	1.00	0.20	1.68	0.16	2.01	0.35	2.45	0.11	2.84	0.18	2.94	0.26	3.17	0.37	3.77	0.22	1.54	0.19
	10^8	1.00	0.24	1.40	0.08	1.30	0.27	1.13	0.22	1.80	0.24	2.14	0.28	2.47	0.44	3.05	0.07	1.48	0.16
	10^9	1.00	0.26	0.98	1.36	1.41	0.50	1.47	0.35	2.42	0.27	1.75	0.34	3.47	0.10	4.13	0.12	1.93	0.19
MHCIα	10^7	1.00	0.33	1.54	0.17	1.31	0.19	2.02	0.21	2.24	0.17	2.92	0.31	2.11	0.46	2.17	0.16	1.81	0.24
	10^8	1.00	0.26	1.61	0.08	1.38	0.21	1.28	0.18	1.40	0.25	2.24	0.49	3.57	0.23	4.07	0.28	1.05	0.17
	10^9	1.00	0.27	1.09	0.06	1.63	0.53	1.47	0.27	1.91	0.19	2.56	0.19	5.04	0.25	5.30	0.15	3.01	0.23

C — Fold changes in the gill

Genes	Groups	0h Fold	0h SEM	3h Fold	3h SEM	9h Fold	9h SEM	15h Fold	15h SEM	24h Fold	24h SEM	36h Fold	36h SEM	48h Fold	48h SEM	72h Fold	72h SEM	96h Fold	96h SEM
CD4-1	10^7	1.00	0.25	2.39	0.04	3.77	0.26	6.14	0.18	5.51	0.31	6.81	0.29	9.43	0.31	4.82	0.12	2.78	0.31
	10^8	1.00	0.36	2.00	0.21	3.06	0.46	5.80	0.37	7.62	0.30	10.53	0.31	13.96	0.11	7.64	0.28	2.06	0.32
	10^9	1.00	0.39	4.73	0.25	7.17	0.30	6.36	0.12	8.07	0.27	12.70	0.67	15.17	0.48	9.25	0.21	6.11	0.25
MHCIIα	10^7	1.00	0.29	1.82	0.24	2.24	0.11	3.34	0.21	4.28	0.30	6.23	0.14	7.92	0.10	6.03	0.22	2.73	0.14
	10^8	1.00	0.18	5.48	0.06	5.82	0.24	6.60	0.29	7.28	0.17	8.21	0.37	14.86	0.29	4.19	0.28	2.82	0.35
	10^9	1.00	0.19	3.06	0.10	3.05	0.27	6.03	0.22	7.11	0.44	9.14	0.47	16.95	0.20	7.13	0.24	3.02	0.23
CD8α	10^7	1.00	0.32	2.55	0.18	2.07	0.13	2.31	0.08	4.46	0.32	5.47	0.17	5.41	0.40	2.05	0.17	3.13	0.12
	10^8	1.00	0.32	2.17	0.11	2.20	0.21	4.03	0.24	6.18	0.18	8.28	0.16	4.82	0.23	4.95	0.37	3.74	0.40
	10^9	1.00	0.18	1.11	0.13	2.01	0.05	6.12	0.61	9.00	0.36	16.04	0.03	9.51	0.17	4.11	0.15	1.58	0.38
MHCIα	10^7	1.00	0.11	1.95	0.26	2.85	0.16	3.51	0.25	4.68	0.35	9.36	0.51	4.05	0.02	2.26	1.69	3.40	0.34
	10^8	1.00	0.23	2.31	0.15	2.63	0.19	2.68	0.22	9.06	0.54	12.41	0.15	5.98	0.24	2.36	0.31	1.97	0.21
	10^9	1.00	0.29	1.39	0.04	2.38	0.46	5.84	0.06	10.63	0.80	17.11	0.05	8.26	0.73	1.54	0.25	1.24	0.11

D — Fold changes in the blood

Genes	Groups	0h Fold	0h SEM	3h Fold	3h SEM	9h Fold	9h SEM	15h Fold	15h SEM	24h Fold	24h SEM	36h Fold	36h SEM	48h Fold	48h SEM	72h Fold	72h SEM	96h Fold	96h SEM
CD4-1	10^7	1.00	0.18	2.42	0.22	3.77	0.20	3.31	0.18	3.61	0.11	5.66	0.15	9.71	0.25	3.03	0.19	2.96	0.32
	10^8	1.00	0.26	3.12	0.30	2.58	0.20	3.74	0.34	5.58	0.37	8.00	0.42	11.60	0.31	7.59	0.33	3.42	0.31
	10^9	1.00	0.17	3.39	0.35	2.87	0.67	6.02	0.07	8.36	0.32	11.55	0.24	15.60	0.12	7.33	0.32	3.43	0.32
MHCIIα	10^7	1.00	0.63	2.59	0.20	1.69	0.36	3.85	0.28	1.71	0.44	5.29	0.07	8.67	0.13	1.41	0.25	5.17	0.41
	10^8	1.00	0.11	2.96	0.09	2.83	0.46	3.42	0.44	5.68	0.21	8.15	0.14	13.42	0.17	6.25	0.19	2.14	0.42
	10^9	1.00	0.27	4.86	0.34	8.65	0.17	11.88	0.12	9.71	0.13	10.56	0.29	16.99	0.16	5.07	0.35	4.65	0.17
CD8α	10^7	1.00	0.34	3.27	0.27	4.06	0.20	4.19	0.24	6.36	0.17	6.88	0.16	8.00	0.12	4.75	0.07	3.85	0.36
	10^8	1.00	0.12	3.10	0.11	3.41	0.21	5.59	0.10	9.13	0.37	12.49	0.37	8.44	0.41	4.15	0.25	3.10	0.26
	10^9	1.00	0.12	3.94	0.40	4.14	0.19	4.26	0.21	2.50	0.11	16.17	0.19	5.22	0.11	3.29	0.28	2.83	0.25
MHCIα	10^7	1.00	0.32	2.12	0.20	2.36	0.32	3.60	0.24	4.29	0.12	7.21	0.16	6.43	0.19	4.44	0.20	2.75	0.20
	10^8	1.00	0.38	3.36	0.17	2.37	0.28	6.26	0.34	11.39	0.24	16.19	0.38	6.77	0.34	2.60	0.26	1.80	0.36
	10^9	1.00	0.19	3.46	0.21	5.58	0.33	5.25	0.23	9.58	0.10	19.37	0.54	11.34	0.25	6.09	0.19	4.80	0.22

Fig. 6. Relative expression of CD4-1, MHC Iα, CD8α and MHC IIα genes in the different tissues of flounder. A. Liver; B. Muscle; C. Gill; D. Blood. The data are presented as the means ± SEM and the length of the color bars indicate the extent of upregulated expressions of the genes. (For interpretation of the references to color in this figure legend, the reader is referred to the Web version of this article.)

take up antigen and present antigen to lymphocytes in order to activate the adaptive immune system [35]. The spleen of teleosts has also been implicated in the clearance and interception of blood-borne particulate material in ellipsoids [36,37]. Therefore, the results indicated that the spleen and head kidney are more efficient to take up antigen and would be the major organs to trap formalin-inactivated *E. tarda* post i.p. injection. This hypothesis was also supported by followed evidences. Previous work found that the head kidney and spleen of Atlantic cod (*Gadus morhua* L.) were the major tissues for taking up the antigen after intraperitoneally injected with *Vibrio anguillarum* [38]. Similar study was also documented that the retention of vaccine components was mainly found in the spleen and kidney of Atlantic salmon (*Salmo salar* L.) after i.p. injection [39].

The immune cells such as lymphocytes, macrophages and granulocytes were reported to be abundant in the mucosal-associated tissues including intestine, skin and gill in teleosts, which play important roles in the antigen presentation and immune response post immersion vaccination [40]. In the present work, a small number of antigen was detected in mucosal-associated tissues post i.p. vaccination, similar results were also found that a small number of ^{3}H-LPS and carbon particles could be detected in the intestine and gill of turbot (*Scophthamus maximus* L) and plaice after i.p. injection [33,41]. It is

speculated that the mucosal tissues could also uptake antigen from the blood circulation and participate in the antigen presentation post i.p. vaccination. In contrast to previous study in which no antigen was detected in the liver of Atlantic Salmon after oral administration with live and inactivated IPNV vaccines [42]. In our study, a large amount of antigen was detected in the liver of flounder after i.p. injection with inactivated *E. tarda*. It is suggested that the liver was also an important organ to take up antigen and the function might be affected by the types, concentration and delivery route of vaccines.

The vaccine concentration is one of the most critical factor for vaccination, which could affect the amount of antigen uptake and the level of immune response, and further had an influence on the vaccination efficacy [16]. In this work, the amount of antigen increased with the increasing concentration of the vaccine in the blood, liver, gill, intestine, skin and muscle, except for the spleen and head kidney, in which more antigen was found in the 10^8 CFU ml^{-1} group than that in the 10^9 CFU ml^{-1} group. It suggested that too high vaccine dose might cause stress to the fish immunity, and the spleen and head kidney might have efflux mediated resistance mechanism to hinder the high dose antigen which uptaking from the blood circulation.

In mammals, the MHC I and MHC II molecule are responsible for presenting the processed antigen to T cells, thus activating the functions of $CD8^+$ and $CD4^+$ T helper cells and forming a bridge between innate and adaptive immune systems [43]. Both MHC class I and class II genes have been reported in a wide variety of teleosts, some of them retained the conserved residues known to bind peptide termini in mammalian MHC sequences, which indicated that similar functions were also present in teleost MHC molecules. Interestingly, the huge MHC class I expansion in Atlantic cod that most likely compensates for the lack of MHC class II and CD4 [44]. In flounder, CD4-1, CD4-2, MHC Iα and MHC IIα genes have been cloned and the functionality of these molecules involving in the presentation and recognition of antigens and immune signal transduction after pathogen invasion in fish were reported by several previous studies [17,40,45–47]. In the present study, the expression of these four antigen presentation genes showed a significant up-regulation in all tested organs after vaccinated with inactivated *E. tarda*, and it is interestingly found that the expression of MHC IIα increased along with MHC Iα, even though the traditional view of antigen presentation stated that intracellular pathogens are presented by MHC I molecules [48]. The result was supported by a previous study in which the expression of MHC Iα in turbot was up-regulated after intraperitoneally injected with formalin-inactivated *E. tarda* [49]. These results might be explained by a fact that presentation of soluble antigens is governed by endocytosis mechanisms, which determined the intracellular routing of the endocytosed antigens. When particulate antigens are internalized into phagosomes, the MHC-I-restricted and MHC-II-restricted presentation will be both initiated [48]. Moreover, the expression of these four genes in the sampled tissues increased in parallel with the increasing of vaccine concentration except for the spleen and head kidney. The differences of the expression levels of these four genes in tissues were in accordance with the dynamic changes of the antigen uptake in different concentration groups. It was found that the increased levels of these antigen presentation related immune genes had a close association with the amount of inactivated *E. tarda* bacterin uptaken in tissues. Generally, higher antigen amount could induce higher expression levels of the four genes in different tested tissues, which suggested that higher amount of antigen uptaken by immune related organs could stimulate stronger immune response of vaccinated fish.

Acknowledgement

This study was supported by the National Natural Science Foundation of China (31730101; 31672685; 31672684; 31472295), the Fundamental Research Funds for the Central Universities (201822015) and Taishan Scholar Program of Shandong Province.

References

[1] W.W. Lee, J.Y. Oh, E.A. Kim, N. Kang, K.N. Kim, G. Ahn, Y.J. Jeon, A prebiotic role of *Ecklonia cava* improves the mortality of *Edwardsiella tarda*-infected zebrafish models via regulating the growth of lactic acid bacteria and pathogen bacteria, Fish Shellfish Immunol. 54 (2016) 620–628.

[2] M.Z. Lan, X. Peng, M.Y. Xiang, Z.Y. Xia, W. Bo, L. He, X.Y. Li, Z.P. Jun, Construction and characterization of a live, attenuated *esrB* mutant of *Edwardsiella tarda* and its potential as a vaccine against the haemorrhagic septicaemia in turbot, *Scophthamus maximus* (L.), Fish Shellfish Immunol. 23 (2007) 521–530.

[3] F.G. Liu, X.Q. Tang, X.Z. Sheng, J. Xing, W.B. Zhan, DNA vaccine encoding molecular chaperone GroEL of *Edwardsiella tarda* confers protective efficacy against edwardsiellosis, Mol. Immunol. 79 (2016) 55–65.

[4] T. Takano, T. Matsuyama, N. Oseko, T. Sakai, T. Kamaishi, C. Nakayasu, M. Sano, T. Lida, The efficacy of five avirulent *Edwardsiella tarda* strains in a live vaccine against edwardsiellosis in Japanese flounder, *Paralichthys olivaceus*, Fish Shellfish Immunol. 29 (2010) 687–693.

[5] M. Yamasaki, K. Araki, K. Maruyoshi, M. Matsumoto, C. Nakayasu, T. Moritomo, T. Nakanishi, A. Yamamoto, Comparative analysis of adaptive immune response after vaccine trials using live attenuated and formalin-killed cells of *Edwardsiella tarda* in ginbuna crucian carp (*Carassius auratus langsdorfii*), Fish Shellfish Immunol. 45 (2015) 437–442.

[6] S.R. Kwon, E.H. Lee, Y.K. Nam, S.K. Kim, K.H. Kim, Efficacy of oral immunization with *Edwardsiella tarda* ghosts against edwardsiellosis in olive flounder (*Paralichthys olivaceus*), Aquaculture 269 (2007) 84–88.

[7] T. Matsuyama, A. Fujiwara, C. Nakayasu, T. Kamaishi, N. Oseko, I. Hirono, T. Aoki, Gene expression of leucocytes in vaccinated Japanese flounder (*Paralichthys olivaceus*) during the course of experimental infection with *Edwardsiella tarda*, Fish Shellfish Immunol. 22 (2007) 598–607.

[8] Y.L. Gao, X.Q. Tang, X.Z. Sheng, J. Xing, W.B. Zhan, Immune responses of flounder *paralichthys olivaceus* vaccinated by immersion of formalin-inactivated *Edward-siella tarda* following hyperosmotic treatment, Dis. Aquat. Org. 116 (2015) 111–120.

[9] T. Ashida, E. Okimasu, M. Ui, M. Heguri, Y. Oyama, A. Amemura, Protection of Japanese flounder *Paralichthys olivaceus* against experimental edwardsiellosis by formalin-killed *Edwardsiella tarda* in combination with oral administration of immunostimulants, Fish. Sci. 65 (1999) 527–530.

[10] J.H.W.M. Rombout, G.W. Yang, V. Kiron, Adaptive immune responses at mucosal surfaces of teleost fish, Fish Shellfish Immunol. 40 (2014) 634–643.

[11] H.M. Munang'andu, B.N. Fredriksen, S. Mutoloki, R.A. Dalmo, Ø. Evensen, Antigen dose and humoral immune response correspond with protection for inactivated infectious pancreatic necrosis virus vaccines in Atlantic salmon (*Salmo salar* L), Vet. Res. 44 (2013) 7.

[12] C.J. Secombes, M.J. Manning, Comparative studies on the immune system of fishes and amphibians: antigen localization in the carp *Cyprinus carpio* L, J. Fish Dis. 3 (1980) 399–412.

[13] A. Eldar, A. Horovitcz, H. Bercovier, Development and efficacy of a vaccine against *Streptococcus iniae* infection in farmed rainbow trout, Vet. Immunol. Immunopathol. 56 (1997) 175–183.

[14] S. Grove, S. Høie, Ø. Evensen, Distribution and retention of antigens of *Aeromonas salmonicida* in Atlantic salmon (*Salmo salar* L.) vaccinated with a Δ aroA mutant or formalin-inactivated bacteria in oil-adjuvant, Fish Shellfish Immunol. 15 (2003) 349–358.

[15] Y. Du, X.Q. Tang, X.Z. Sheng, J. Xing, W.B. Zhan, Immune response of flounder (*Paralichthys olivaceus*) was associated with the concentration of inactivated *Edwardsiella tarda* and immersion time, Vet. Immunol. Immunopathol. 167 (2015) 44–50.

[16] Y. Du, X.Q. Tang, X.Z. Sheng, J. Xing, W.B. Zhan, The influence of concentration of inactivated *Edwardsiella tarda* bacterin and immersion time on antigen uptake and expression of immune-related genes in Japanese flounder (*Paralichthysolivaceus*), Microb, Pathogens 103 (2017) 19–28.

[17] Y.L. Gao, X.Q. Tang, X.Z. Sheng, J. Xing, W.B. Zhan, Antigen uptake and expression of antigen presentation-related immune genes in flounder (*paralichthys olivaceus*) after vaccination with an inactivated *Edwardsiella tarda,* immersion vaccine, following hyperosmotic treatment, Fish Shellfish Immunol. 55 (2016) 274–280.

[18] X.H. Liu, H.Z. Wu, X.Y. Chang, Y.F. Tang, Q. Liu, Y.X. Zhang, Notable mucosal immune responses induced in the intestine of zebrafish (*Danio rerio*) bath-vaccinated with a live attenuated *Vibrio anguillarum* vaccine, Fish Shellfish Immunol. 40 (2014) 99–108.

[19] U. Khimmakthong, S. Deshmukh, J.K. Chettri, A.M. Bojesen, P.W. Kania, I. Dalsgaard, K. Buchmann, Tissue specific uptake of inactivated and live *Yersinia ruckeri* in rainbow trout (*Oncorhynchus mykiss*): visualization by immunohistochemistry and *in situ* hybridization, Microb. Pathog. 59–60 (2013) 33–41.

[20] M. Ototake, T. Nakanishi, Kinetics of bovine serum albumin in fish plasma after hyperosmotic infiltration treatment: comparison between marine and freshwater fish, Aquaculture 103 (1992) 229–240.

[21] E.M. Crump, M.B. Perry, S.C. Clouthier, W.W. Kay, Antigenic characterization of the fish pathogen *Flavobacterium psychrophilum*, Appl. Environ. Microbiol. 67 (2001) 750–759.

[22] J.L. Fryer, R.P. Hedrick, *Piscirickettsia salmonis*: a Gram-negative intracellular bacterial pathogen of fish, J. Fish Dis. 26 (2003) 251–262.

[23] N. Budimir, A. Huckriede, T. Meijerhof, L. Boon, E. Gostick, D.A. Price, J. Wilschut, A. de Haan, Induction of heterosubtypic cross-protection against influenza by a whole inactivated virus vaccine: the role of viral membrane fusion activity, PLoS One 7 (2012) e30898.

[24] M. Ohtani, K.R. Villumsen, H.K. Strøm, M.K. Raida, 3D Visualization of the initial *Yersinia ruckeri* infection route in rainbow trout (*Oncorhynchus mykiss*) by optical projection tomography, PLoS One 9 (2014) e89672.
[25] C.C. Labarca, M. Makhutu, A.E. Lumsdon, K.D. Thompson, R. Jung, W. Kloas, K. Knopf, The adjuvant effect of low frequency ultrasound when applied with an inactivated *Aeromonas salmonicida* vaccine to rainbow trout (*Oncorhynchus mykiss*), Vaccine 33 (2015) 1369–1374.
[26] X.Q. Tang, W.B. Zhan, X.Z. Sheng, H. Chi, Immune response of Japanese flounder *Paralichthys olivaceus* to outer membrane protein of *Edwardsiella tarda*, Fish Shellfish Immunol. 28 (2010) 333–343.
[27] S.R. Hong, S.J. Choi, H.D. Jeong, S. Hong, Development of QCM biosensor to detect a marine derived pathogenic bacteria *Edwardsiella tarda* using a novel immobilisation method, Biosens. Bioelectron. 24 (2009) 1635–1640.
[28] K.J. Livak, T.D. Schmittgen, Analysis of relative gene expression data using real-time quantitative PCR and the $2^{-\Delta\Delta CT}$ method, Methods 25 (2001) 402–408.
[29] S.R. Lill, R.H. Parsons, I. Buhac, Permeability of the diaphragm and fluid resorption from the peritoneal cavity in the rat, Gastroenterology 76 (1979) 997–1001.
[30] M.F. Abu-Hijleh, O.A. Habbal, S.T. Moqattash, The role of the diaphragm in lymphatic absorption from the peritoneal cavity, J. Anat. 186 (1995) 453.
[31] H. Ellens, H. Morselt, G. Scherphof, In vivo fate of large unilamellar sphingomyelin-cholesterol liposomes after intraperitoneal and intravenous injection into rats, Biochim. Biophys. Acta Gen. Subj. 674 (1981) 10–18.
[32] C.R. Tyler, J.P. Sumpter, N.R. Bromage, In vivo ovarian uptake and processing of vitellogenin in the rainbow trout, *Salmo gairdneri*, J. Exp. Zool. 246 (1988) 171–179.
[33] A.E. Ellis, A.L.S. Munroe, R.J. Roberts, Defence mechanisms in fish, J. Fish Biol. 8 (1976) 67–78.
[34] C.M. Press, O. Evensen, The morphology of the immune system in teleost fishes, Fish Shellfish Immunol. 9 (1999) 309–318.
[35] C. Agius, R.J. Roberts, Melano-macrophage centres and their role in fish pathology, J. Fish Dis. 26 (2003) 499–509.
[36] A. Espenes, C.M. Press, B.H. Dannevig, T. Landsverk, Immune-complex trapping in the splenic ellipsoids of rainbow trout (*Oncorhynchus mykiss*), Cell Tissue Res. 282 (1995) 41–48.
[37] M.G. Maas, R. Bootsma, Uptake of bacterial antigens in the spleen of carp (*Cyprinus carpio* L.), Dev. Comp. Immunol. 2 (1982) 47–52.
[38] S.M. Arnesen, M.B. Schroder, R.A. Dalmo, J. Bogwald, Antigen uptake and immunoglobulin production in Atlantic cod (*Gadus morhua L.*) after intraperitoneal injection of *Vibrio anguillarum*, Fish Shellfish Immunol. 13 (2002) 159–170.
[39] C.M. Press, Ø. Evensen, L.J. Reitan, T. Landsverk, Retention of furunculosis vaccine components in Atlantic salmon, *Salmo salar* L., following different routes of vaccine administration, J. Fish Dis. 19 (1996) 215–224.
[40] G. Kato, T. Takano, T. Sakai, T. Matsuyama, C. Nakayasu, *Vibrio anguillarum* bacterin uptake via the gills of Japanese flounder and subsequent immune responses, Fish Shellfish Immunol. 35 (2013) 1591–1597.
[41] R.A. Dalmo, T. Seternes, S.M. Arnesen, T.O. Joergensen, J. Bøgwald, Tissue distribution and cellular uptake of *Aeromonas salmonicida* lipopolysaccharide (LPS) in some marine fish species, J. Fish Dis. 21 (1998) 321–334.
[42] L. Chen, Ø. Evensen, S. Mutoloki, IPNV antigen uptake and distribution in Atlantic salmon following oral administration, Viruses 7 (2015) 2507–2517.
[43] T. Storni, M.F. Bachmann, Loading of MHC class I and II presentation pathways by exogenous antigens: a quantitative in vivo comparison, J. Immunol. 172 (2004) 6129–6135.
[44] U. Grimholt, MHC and evolution in teleosts, Biology 5 (2016) 6.
[45] P. Srisapoome, T. Ohira, I. Hirono, T. Aoki, Cloning, characterization and expression of cDNA containing major histocompatibility complex class I, IIα and IIβ genes of Japanese flounder *Paralichthys olivaceus*, Fish. Sci. 70 (2004) 264–276.
[46] F.G. Liu, X.Q. Tang, X.Z. Sheng, J. Xing, W.B. Zhan, Comparative study of the vaccine potential of six outer membrane proteins of *Edwardsiella tarda* and the immune responses of flounder (*Paralichthys olivaceus*) after vaccination, Vet. Immunol. Immunopathol. 185 (2017) 38–47.
[47] K. Zhu, W. Yu, H. Guo, N. Zhang, S. Jiang, D. Zhang, The polymorphisms of MHCIIß gene of Trachinotus ovatus and their association with resistance/susceptibility to Photobacterium damsela, Aquaculture 485 (2018) 160–165.
[48] S. Burgdorf, S. Kurts, Endocytosis mechanisms and the cell biology of antigen presentation, Curr. Opin. Immunol. 20 (2008) 89–95.
[49] X. Liu, H. Zhang, C. Jiao, Q. Liu, Y. Zhang, J. Xiao, Flagellin enhances the immunoprotection of formalin-inactivated *Edwardsiella tarda* vaccine in turbot, Vaccine 35 (2017) 369–374.